*Revised Manuscript
Click here to view linked References

Transcriptome profiling, and cloning and characterization of the main monoterpene synthases of *Coriandrum sativum* L.

Authors: Mariana Galata[a], Lukman S. Sarker[a], Soheil S. Mahmoud[a*]

a Department of Biology, University of British Columbia Okanagan Campus, 3333 University Way, Kelowna, BC, Canada V1V 1V7

Corresponding author: Soheil S. Mahmoud, (250) 807-8752, soheil.mahmoud@ubc.ca

ABSTRACT Terpenoids are a large and diverse class of specialized metabolites that are essential for the growth and development of plants, and have tremendous industrial applications. The mericarps of *Coriandrum sativum* L. (coriander) produce an essential oil (EO) rich in monoterpenes, volatile C_{10} terpenoids. To investigate EO metabolism, the transcriptome of coriander mericarps, at three developmental stages (early, mid, late) was sequenced via Illumina technology and a transcript library was produced. To validate the usability of the transcriptome sequences, two terpene synthase candidate genes, *CsγTRPS* and *CsLINS*, encoding 558 and 562 amino acid proteins were expressed in bacteria, and the recombinant proteins purified by Ni-NTA affinity chromatography. The 65.16 (CsγTRPS) and 65.91 (CsLINS) kDa recombinant proteins catalyzed the conversion of geranyl diphosphate, the precursor to monoterpenes, to γ-terpinene and (S)-linalool, respectively, with apparent V_{max} and K_m values of 2.24±0.16 (CsγTRPS); 19.63±1.05 (CsLINS) pkat/mg and 66.25 ± 13 (CsγTRPS); 2.5±0.6 (CsLINS) μM, respectively. Together, CsγTRPS and CsLINS account for the majority of EO constituents in coriander mericarps. Investigation of the coriander transcriptome, and knowledge gained from these experiments will facilitate future studies concerning essential and fatty acid oil production in coriander. They also enable efforts to improve the coriander oils through metabolic engineering or plant breeding.

Keywords: Coriander; *Coriandrum sativum*; Apiaceae; Transcriptome; Monoterpenes; (S)-Linalool synthase; γ-Terpinene synthase

1. Introduction

Coriandrum sativum (coriander) is a hardy annual plant belonging to the *Apiaceae* family, today cultivated in various temperate countries. The term cilantro refers to its leaf tissue, while the dry fruits are known as coriander mericarps (Reuter et al., 2008). Coriander mericarp oil is comprised of both fatty acids, as well as essential oil (EO); the leaves do not produce any EO. Lipid content of coriander mericarp oil is high, 28.4% of the total mericarp weight, which may be of great importance in the food industry (Ramadan and Morsel, 2002). Its EO has been shown to exhibit antimicrobial, anti-inflammatory and anti-hyperglycemic properties, to name a few (Gallagher et al., 2003; Kubo et al., 2004; Reuter et al., 2008).

Plant terpenoids, or isoprenoids, are made up of five carbon isoprene units, and are found in all plant tissues including leaves, flowers, buds, stems, roots, and seeds. Due to the cytotoxicity of many terpenoids (those which constitute EOs), plants have developed certain specialized structures for storage of these compounds. For example, flowers store terpenoids in glandular trichomes, while mericarps do so in secretory canals called vittae (Gross et al,, 2006). In plants, terpenoids perform a variety of essential functions in growth and development (e.g., as growth regulators) and have crucial ecological roles (e.g., in defense and pollinator attraction) (Bakkali et al., 2008). These compounds are valuable in many industries, for example, medicine, agriculture (e.g., as pesticides), culinary (e.g., as flavorants) and hygiene (e.g., in scented products) (Chithra and Leelama, 2000; Gallagher et al., 2003; Kubo et al., 2004; Lo Cantore et al., 2004).

There are seven major classes of terpenoids, categorized according to the number of isoprene units that make up their backbone structure (Buchanan et al., 2002; Yazaki, 2006). These include the mono- (C_{10}), sesqui- (C_{15}), di- (C_{20}), sester- (C_{25}), tri-(C_{30}), tetra- (C_{40}), and polyterpenes (C_n). These natural products are biosynthesized via two distinct pathways in separate cellular compartments. The 1-deoxyxylulose-5-phosphate (DXP) pathway is located in the plastid, and through this pathway, mono-, di-, and tetra-terpenes are produced (Hasunuma, et al., 2008; Rodriguez-Concepcion, 2010). The mevalonate (MVA) pathway operates in the cytosol, where it is responsible for the production of sesqui-, tri-, and poly-terpenes (Ganjewala et al., 2009; Rodriguez-Concepcion, 2010). Each of these pathways yields universal terpenoid precursors, isopentenyl diphosphate (IPP) and its allylic isomer dimethylallyl diphosphate (DMAPP). Further condensation of these two terpenoid precursors gives rise to prenyl diphosphates, geranyl diphosphate (GPP), farnesyl diphosphate (FPP) and geranyl geranyl diphosphate (GGPP) (Supplementary Figure S1), the linear precursors to various isoprenoids. Specialized enzymes known as terpene synthases/cyclases convert these substrates to the great variety of terpenoids found in plants. Numerous terpenoids can be further modified via both enzymatic and non-enzymatic processes to increase plant terpene diversity (Mahmoud and Croteau, 2002; Rodriguez-Concepcion, 2010).

Coriander EO is a blend of mainly monoterpenes, as well as a small number of sesquiterpenes. (S)-Linalool (**1**) is the most abundant monoterpene found in coriander EO, making up approximately 72% of the oil. The mericarp EO composition changes as the mericarp matures; monoterpene alcohols (e.g., (S)-linalool (**1**)) increase, while monoterpene hydrocarbons, esters and ketones decrease (Msaada et al., 2009a).

Previous studies on coriander have primarily focused on fatty acid biosynthesis and essential oil composition; however, coriander mericarp EO biosynthesis remains understudied, and the terpene synthases responsible for monoterpene production in this plant have not been described. The main objective of the work presented here was to clone and functionally characterize the main coriander terpene synthases, in particular (S)-linalool synthase, which is responsible for the production of (S)-linalool (**1**), the main component of coriander EO.

Given that the production of several monoterpenes is regulated, at least in part, at the transcriptional level (Lane et al., 2010), it was anticipated herein that transcript levels for (S)-linalool synthase would also increase as coriander mericarps mature. Illumina sequencing technology was thus used to obtain sequence information for the entire transcriptome of the *C. sativum* mericarp across three developmental stages (early, mid and late). This information facilitated cloning of terpene synthases from coriander, and enabled investigation of expression patterns of two key regulatory genes, DXP synthase (DXS) and HMG-CoA reductase (HMGR), in isoprenoid biosynthesis.

The sequence information obtained from this study will aid in novel gene discovery and for development of molecular markers for improvement of *C. sativum* through plant breeding. Additionally, knowledge regarding EO biosynthesis in coriander mericarps may aid future efforts to improve plant mericarp EO content via genetic engineering. Mericarps are excellent storage vessels, as they maintain oil integrity and have minimal storage requirements (Misharina, 2001). This makes plant mericarps great targets for research concerning production of industrially valuable terpenoids.

2. Results and discussion

2.1. Scanning Electron Microscopy (SEM)

High resolution images were obtained of coriander whole mericarp and cross-section (Fig. 1A and B). Four vittae, or secretory canals, are clearly visible in Fig. 1B and a close-up in Fig. 1D. These vittae are the storage sites of coriander mericarp EOs (Parthasarthy and Zachariah, 2008; Purseglove et al., 1981), unlike some angiosperms which store EOs in glandular trichomes (Turner and Croteau, 2004) and gymnosperms which store EOs in resin ducts (Wu and Hu, 1997). Typical stomata, complete with guard cells, are present on the surface of the coriander mericarp (Fig. 1C). The presence of stomata on mericarps is uncommon, although it has been previously reported (e.g., in *Bauhinia* and *Eschscholzia*) (Jernstedt and Clark, 1979; Rugenstein and Lersten, 1981).

To date, the exact function of stomata on plant mericarps has not been elucidated with certainty. Proposed functions include facilitation of gas exchange in photosynthesizing mericarps, during embryo development, as well as playing a role during imbibition (Jernstedt and Clark, 1979; Paiva et al., 2006; Werker, 1997). Green plant tissues, including green plant mericarps, have entered the greening process and are actively photosynthesizing (Tschiersch et al., 2011). According to the RNA-seq data, coriander mericarps strongly express all photosynthetic genes (Supplementary Table S1). This, coupled with the observation that developing coriander mericarps are green, indicates that these tissues are actively photosynthesizing during their development. Once coriander mericarps have matured and fallen from the parent plant they become desiccated and their seed coat browns and hardens. Photosynthesis is likely inactive at this point yet the stomata may still function in imbibition, allowing water to enter the seed to initiate germination.

2.2 Essential oil analysis of C. sativum mericarps

Analysis of the EO steam distilled from *C. sativum* mericarps established that, as previously reported (Bhuiyan, 2009; Misharina, 2001; Msaada, 2009a; Potter, 1996; Sriti, 2009), the major component of this EO is (S)-linalool (**1**). After (S)-linalool (**1**), mericarps from the *C. sativum* plants used in this study were most abundant in cymene (**2**), ocimene (**3**), camphor (**4**) and γ-terpinene (**5**), listed in order of abundance. Those volatile terpene products present in amounts less than 2% of total EO terpenes include limonene (**6**), linalool oxide (**7**), geraniol (**8**), β-phellandrene (**9**), sabinene (**10**), camphene (**11**), terpinene-4-ol (**12**), borneol (**13**), α-terpineol (**14**), terpinolene (**15**), 1,8-cineole (**16**) and citronellene (**17**) (Table 1, Fig. 2).

2.3. Transcriptome Sequencing and Annotations

Transcriptome sequencing yielded a total of 33,330,312 raw reads of 65bp length each, 10,638,013 from Sample 1 (S1; small mericarps), 12,513,426 from Sample 2 (S2; medium mericarps) and 10,178,873 from Sample 3 (S3; large mericarps). *De novo* assembly yielded 65,306 transcripts of a median length of 519 bp. All unique transcript sequences were aligned against sequences in The Arabidopsis Information Resource TAIR (v.2.2.8) and UniProtKB databases, resulting in 55,689 sequences with blast hits.

Of the 65,306 transcripts, 35,928 were assigned at least one gene ontology (GO) term. Among these, 26,882 (41.16%), 19,025 (29.13%) and 32,405 (49.62%) sequences were assigned at least one GO term in the biological processes, cellular component and molecular function categories, respectively. Distribution of the most abundant GO terms for biological processes, molecular functions, and cellular components is summarized in Supplementary Figure S2. Transcript sequences with no BLASTx hits are likely novel and involved in functions specific to *C.*

sativum. The study of these genes may lead to uncovering evolutionary or species-specific processes including adaptation and speciation.

KEGG annotations categorized 1508, 760 and 442 transcripts under metabolism, genetic information processing and cellular processes, respectively. Within those transcripts grouped under metabolism, 287 corresponded to carbohydrate metabolism, 235 to amino acid metabolism, 197 to lipid metabolism (includes all genes involved in fatty acid biosynthesis/metabolism), 189 to energy metabolism, 179 to secondary products metabolism (includes all genes involved in terpenoid, phenylpropanoid, flavonoid, alkaloid and polyketide metabolism), 151 to nucleotide metabolism, 101 to cofactors/vitamins metabolism and 169 to other processes (e.g., other amino acids and glycan metabolism) (Supplementary Figure S3 and Supplementary Table S2).

Novel full-length protein and nucleotide sequences of CsγTRPS and CsLINS generated for this study were deposited in Genbank with the following accession numbers KF700699 and KF700700, respectively.

2.4. Terpene Biosynthetic Gene Expression Analysis

Differential transcript abundance data for each of the DXP and MVA pathway genes, as well as related prenyl transferases and other terpene biosynthetic genes, are represented in Table 2 and Supplementary Table S3. The data was analyzed using Reads Per Kilobase per Million mapped reads (RPKM), and thus data in Table 2 and Supplementary Table S3 are represented as RPKM-normalized counts. The fold change (differential expression) is represented by $\log_2$ ratio transformations. A negative $\log_2$ ratio represents down-regulation, a positive value, up-regulation and a ratio of 0 is indicative of no differential expression between two samples.

Transcripts for DXS and HMGR, which are considered key regulatory enzymes in EO biosynthesis (Munoz-Bertomeu et al., 2006; Rodriguez-Concepcion, 2010) demonstrated relatively constant levels of transcript abundance throughout mericarp development, with the exception of DXS2 which exhibited an approximately 2-fold decrease in transcript abundance from S2 to S3. Further, transcripts for all isoprenoid synthesis-related prenyl transferase genes were present.

In coriander, because the EO is vastly dominated by monoterpenes, rather than sesquiterpenes (Msaada et al., 2009a), it is likely that farnesyl diphosphate synthase (FPPS) feeds the biosynthesis of large amounts of non-EO related metabolites such as triterpenes, which are also derived from farnesyl diphosphate (FPP). All plants generate triterpenes, many of which are precursors to important plant sterols and other growth regulators (Benveniste, 2004; Clouse and Sasse, 1998). The high GGPPS transcript expression suggests that coriander mericarps also produce tetraterpenes, which are commonly found in plant mericarps as precusors to important growth regulators, photoprotective quenching compounds and as accessory pigments in the photosynthetic system (Maluf et al., 1997).

In a study by Lane et al., 2010, it was found that *Lavandula angustifolia* flowers exhibit clear differential expression of the DXS and HMGR genes with DXS expressing 7-fold more than HMGR, leading to the conclusion that the flower terpene content was primarily produced via the DXP pathway. The mericarps of *C. sativum* exhibit a relatively constant and constitutive pattern of both DXS and HMGR gene expression, with DXS more strongly expressed (2-fold) than HMGR. This suggests that, like in *L. angustifolia* flowers, in *C. sativum* mericarps, terpene content of the EOs are primarily produced through the DXP pathway. However, differential expression between DXS and HMGR genes was not as pronounced in coriander mericarps as

was the case in the lavender flowers, suggesting that the MVA pathway may also contribute to EO production in coriander. This would occur via metabolic exchange of the phorphorylated intermediates (IPP and DMAPP) between the plastid and cytosol (Hemmerlin et al., 2003).

Upon analyzing the transcript abundance of terpene synthase genes (Table 2), it was found that there were many tetraterpene biosynthetic genes actively expressed in the coriander mericarp, which correlated with the high expression of GGPPS. The majority of these genes (57%) exhibited peak expression at S3. The two most abundantly expressed tetraterpene genes, 15-cis-phytoene desaturase and zeaxanthin epoxidase are involved in β-carotene and abscisic acid biosynthesis, respectively. Genes involved with diterpene production had substantially lower transcript abundance than tetraterpene biosynthetic genes. The two diterpene biosynthetic genes with greatest expression are directly involved in gibberellin biosynthesis, diterpene-derived plant hormones which play roles in fruit/seed senescence.

Two putative sesquiterpene synthase genes (sTPS1 and sTPS2) were identified that, according to GO annotations, encoded for enzymes responsible for the production of β-caryophyllene, α-humulene, and germacrene D. Both genes were KEGG annotated as part of the β-caryophyllene and α-humulene biosynthetic pathways. Given that coriander EO containes all three sesquiterpenes, it is likely that one or both of those genes predominantly converts FPP to more than one of those three sesquiterpenes; more work is required to conclusively establish this.

Transcript levels for the (S)-linalool synthase gene were the most abundant of the four mTPS candidates, and peaked at S2 (2-fold upregulation from S1 to S2 and 5-fold downregulation from S2 to S3). In addition to the high levels of the (S)-linalool synthase transcript in coriander, another likely reason for the large amount of linalool **(1)** content in coriander EO by late maturity is due to accumulation of the monoterpene over time, rather than increased (S)-linalool synthase

expression at S3. In the case of γ-terpinene synthase, transcript abundace also peaked at S2 but did not parrallel γ-terpinene oil content, which dips lowest at middevelopment. This may be due to the various factors involved with post-transcriptional and post-translational regulation of EO biosynthetic genes. It is known that transcriptome sequencing data only suggest changes in the transcript abundance, and does not necessarily represent "protein levels" since translation to active protein may be post-transcriptionally and post-translationally regulated (Barrett et al., 2005; Valasek and Repa, 2005).

Given that 17 monoterpenes were identified in *C. sativum* mericarp EO, and only 4 mTPS candidate genes were identified in this study, it is likely that as with many plant TPSs, coriander terpene synthases are multiproduct enzymes that can produce several monoterpene products from a single GPP substrate.

2.5. CsγTRPS and CsLINS Candidate Gene Selection

Transcripts with the GO annotation "monoterpene biosynthetic process", as well as transcripts with BLASTx hits to known mono-TPS genes having a cutoff e-value of $<10^{-60}$ were selected as putative coriander mTPS gene candidates. Two of these candidates, *CsγTRPS* and *CsLINS*, were chosen based on sequence homology to known mTPS genes, especially the presence of conserved motifs shared by all known TPS genes, DDXXD, (N,D)D(L,I,V)X(S,T)XXXE and RRX_8W, as well as one partially conserved motif, LQLYEASFLL. Protein sequence alignments between *CsγTRPS*, *CsLINS* and *Citrus limon* γ-terpinene synthase (E2E2P0.1), *Lavandula angustifolia* linalool synthase (ABB73045.1), *Salvia fruticosa* 1,8-cineole synthase (ABH07677.1), *Cannabis sativa* limonene synthase (ABI21837.1), *L. angustifolia* β-phellandrene synthase (ADQ73631.1) and *Salvia officinalis* sabinene synthase (AAC26018.1) were performed with ClustalW2 (Supplementary Figure S4). This analysis indicated that

CsγTRPS and *CsLINS* contained all highly conserved motifs found in monoterpene synthases including the RRx8W motif involved in cyclization of the GPP substrate, the DDxxD and (N,D)D(L,I,V)x(S,T)xxxE motifs involved in divalent metal ion coordination, and the LQLYEASFLL motif involved in substrate binding (Supplementary Figure S4). Sequence alignment via the BLASTx algorithm against NCBI non-redundant protein sequences demonstrated *CsγTRPS* to share 49% conserved identity with γ-terpinene synthase from *Citrus unshiu* (BAD27259.1), and CsLINS to share 51% conserved identity with (d)-limonene synthase from *Citrus unshiu* (BAD27257.1).

2.6. Bacterial Expression and Functional Characterization of CsγTRPS and CsLINS

The N-terminal signal peptide of TPSs, which is necessary for the pseudo-mature TPS to be transported to the plastid, where it becomes fully mature mono-TPS, has been found to render TPSs expressed in bacteria insoluble, thus inactive. Therefore, the signal peptides are generally eliminated from mono-TPS gene sequences during cloning work (Vonheijne and Steppuhn, 1989). The complete ORF of *CsγTRPS* and CsLINS were 1,833 bp and 1773 bp, of which 186 bp and 114 bp corresponding to the putative signal peptides, were removed to improve protein solubility during expression. The truncated genes tagged with eight C-terminal histidine residues encoded a 558 and 562 amino acid proteins for CsγTRPS and CsLINS, respectively, with predicted masses of 65.16 and 65.91 kDa. The ORFs of *CsγTRPS* and *CsLINS*, excluding the transit peptides, were expressed in bacterial cells and the recombinant proteins purified and assayed for activity with GPP. Incubation of the bacterially produced CsγTRPS with GPP (**18**) yielded γ-terpinene (**5**) as major product (91.1%) in addition to a number of minor products, including sabinene (**10**) (6.97%), α-terpinene (**19**) (1.18%), terpinene-4-ol (**12**) (0.533%), and α-terpineol (**14**) (0.246%) (Fig. 3 and Supplementary Figure S5). Incubation of bacterially

produced CsLINS with GPP (**18**) yielded a single product, (S)-linalool **(1)** (Fig. 3). The stereoisomerism of (S)-linalool **(1)** was confirmed by gas chromatography using a chiral column (Agilent, Missisauga, ON, CAN) (Fig. 4). In Figure 5C, there is a slight (R)-linalool (20) peak in addition to the (S)-linalool **(1)** peak. This (R)-linalool (**20**) presence is likely due to solvolysis of the GPP substrate, the stock of which was made up in water. Coriander EO contains only the (S) isomer of linalool **(1)**, as opposed to the lavender flowers previously studied by Lane et al., 2010, which only produce the (R) isomer (20). In future, work could be done to investigate the structural reason behind the stereospecificity of these linalool synthases. Together CsγTRPS and CsLINS describe the majority of coriander's EO terpenoid content.

The linear kinetics ranged from 2.5 to 15 (CsγTRPS) and 10 to 90 (CsLINS) minutes. The optimum pH for both CsγTRPS and CsLINS ranged from 6.0 – 6.5, while the optimum temperature ranged from 30 – 35 ºC with a slight activity peak at 32 ºC (CsγTRPS), 33 ºC (CsLINS). The Michaelis-Menten enzyme saturation curve was prepared for each enzyme using the hyperbolic enzyme analysis module in the SigmaPlot software (v.10.0) (Systat Software, Erkrath, Germany) (Fig. 5A and B). The K_m, V_{max} and catalytic efficiency for CsγTRPS were calculated to be 66.25 ± 13.32 μM, 2.24 ± 0.16 p_{kat}/mg and 2.228×10^{-6} $s^{-1}\mu M^{-1}$, respectively; and these parameters for CsLINS were 2.5 ± 0.63 μM, 19.63± 1.05 p_{kat}/mg and 5.40×10^{-4} $s^{-1}\mu M^{-1}$, respectively. From these values, it can be seen that CsγTRPS had a low affinity for its substrate, GPP **(18)**, and was saturated at a low substrate concentration, while CsLINS was saturated at a substrate concentration 10-fold higher than CsγTRPS and its affinity for GPP was much greater than was the case with CsγTRPS. Turnover and efficiency data shown in Table 3 for CsγTRPS and CsLINS indicate that the catalytic efficiency of CsγTRPS is much less than observed in CsLINS. It is expected that CsγTRPS be a slower enzyme than CsLINS because, γ-terpinene **(5)**

is only a minor component of coriander EO while (S)-linalool (**1**) makes up approximately 79% of the total EO terpene content (Table 1). These data do not exclude other possible regulatory elements that determine the composition of coriander EO. No enzymatic activity was detected upon incubation with FPP. The major product of CsγTRPS, γ-terpinene (**5**), is a precursor of the second most abundant monoterpene in the *C. sativum* mericarps used for this study, cymene (**2**) (6.38% of total EO terpene content) (Poulose and Croteau, 1978). Oxygenation of γ-terpinene (**5**) carried out by cytochrome p450 mono-oxygenases is likely responsible for the conversion of γ-terpinene (**5**) to cymene (**2**) in these mericarps, as has been shown to be the case in other plants (Lupien et al., 1999). Camphor (**4**), the fourth most abundant monoterpene in the mericarps used here (3.62% total EO terpene content), is the product of a borneol dehydrogenase, converting borneol (**13**) to camphor (**4**), rather than the action of a monoterpene synthase (Okamoto et al., 2011; Sarker et al., 2012). Thus, the two monoterpene synthases CsLINS and CsγTRPS are together responsible for the biosynthesis of the most abundant EO constituents ((S)-linalool (**1**), γ-terpinene (**5**), and cymene (**2**)) and produce the bulk of the EO in the *C. sativum* mericap.

3. Conclusions

C. sativum is both an important culinary herb and EO crop. Coriander EO has been shown to exhibit medicinal activity, for example as an anti-hyperlipedemic and an anxiolytic (Dhanapakiam et al., 2008; Mahendra and Bisht, 2011). Further, coriander mericarps contain large quantities of the monounsaturated fatty acid, petroselinic acid which is useful in the production of detergents and nylon polymers (Msaada et al., 2009b). Although coriander is clearly an important crop, genomic resources for this plant have not been developed. This study is the first to develop a transcript library for coriander and to clone two mTPS genes which make up the majority of the total EO monoterpene content in this plant.

In addition to facilitating gene discovery, the de novo transcriptome assembly of this non-model plant contributes to the advancement of genetics and plant breeding research for this underutilized crop. For example, the genetic composition and gene functionality information provided by this research can lead to identification of molecular markers such as STRs and SNPs (Li et al., 2012; Li et al., 2013). Also, future development of molecular markers will allow this specialty oil crop plant to be industrially improved via marker-assisted selective breeding. Finally, these results can be used to improve oil yield and quality of coriander through metabolic engineering.

4. Experimental

4.1. Plant Material

C. sativum seeds were germinated and plants grown in growth chamber at 25 ºC and 150 µmol m^{-2} s^{-1} light intensity, with a 16:8 photoperiod, until plants were bearing mericarps of varying maturity levels. Mericarps of three distinct size (maturity) stages, small (1-2.5 mm diameter) – sample 1, medium (2.5-4 mm diameter) – sample 2, and large (>4 mm diameter) – sample 3, were harvested and immediately frozen in N_2 and stored at -80ºC.

4.2. Scanning Electron Microscopy (SEM)

Large coriander mericarps were submersed in N_2 before being cross-sectioned for SEM. Both whole and cross-sectioned mericarps were coated with 7.5 nm of a palladium-platinum alloy using a Cressington Sputter Coater 208HR and Thickness Controller MTM20 (Cressington Scientific Instruments Ltd., Watford, England). SEM imaging was performed on a Tescan Mira3 XMU Field Emission Scanning Electron Microscope (TESCAN, Brno, Czech Republic).

4.3. Analysis of C. sativum essential oil

C. sativum EO was extracted from 0.80 g of a blend of 1-4.5 mm diameter mericarps. The EO was distilled for 45min in pentane (10 ml) containing 10 mg/ml menthol (10 µl) as internal standard using a Clevenger-type apparatus. The organic layer was collected at room temperature and atmospheric pressure. The oil was analyzed by gas chromatography-mass spectrometry (GC-MS) using a Varian GC 3800 Gas Chromatographer coupled with a Saturn 2200 Ion Trap mass detector as previously described (Demissie et al., 2011). The GC was equipped with a 30 m × 0.25 mm capillary column coated with a 0.25 µm film of acid-modified polyethylene glycol (ECTM 1000, Altech, Deerfield, IL, USA); as well as a CO_2 cooled 1079 Programmable Temperature Vaporizing (PTV) injector (Varian Inc., USA). Two microliter concentrated samples were injected at 40 ºC. The oven temperature was initially maintained at 40 ºC for 3 minutes, followed by a two-step temperature increase, first to 130 ºC (ramp rate of 10 ºC per minute) and then to 230 ºC (ramp rate of 50 ºC per minute), and held at 230 ºC for 8 minutes. The helium carrier gas flow rate was 1 ml per minute. Essential oil volatile products were identified by comparison of their retention times and mass spectra to those of authentic standards (when available), or to those in the National Institute of Standards and Technology (NIST) library database (NIST MS Search v.2.0). Two separate 0.80 g batches of *C. sativum* mericarps were steam distilled simultaneously and each extract was injected twice through the GC-MS.

4.4. RNA Isolation and Quality Controls

Total RNA was extracted from the three developmental samples (S1, S2 and S3) of *C. sativum* mericarps. The RNA was extracted using an Omega E.Z.N.A Plant RNA Kit, including DNase 1 digestion following exactly the protocol recommended by the manufacturer (OMEGA bio-tek, GA, USA). The RNA was quantified and its purity determined using a UV-Vis

spectrophotometer (Nanodrop ND-100, Wilmington, DE, USA) and its integrity was assessed on a 1.5% agarose gel.

4.5. Transcriptome Sequencing and De Novo Assembly

Complementary DNA was generated for each mericarp RNA sample and the transcriptome of the three multiplexed samples were single-end sequenced on a single flow cell lane using an Illumina GAIIx sequencer (Illumina Inc., San Diego, CA, USA). Raw reads obtained from the Illumina genome analyzer were searched for adapters and quality trimmed using Btrimm. The individual reads were then each broken down into three different k-mer length fragments: 21, 27, and 31, so that they could be assembled into contigs (three different contig libraries) via the de Bruijn graph algorithms in the publicly available Velvet software (v.1.0). The resulting contig libraries became the input for the also publicly available Oasis transcript assembler with default settings (initial release). The sequencing and library construction were performed by service providers at the Plant Biotechnology Laboratory, University of Lethbridge (Lethbridge, AB, CA).

4.6. Bioinformatics

Using the BLASTx algorithm, *C. sativum* transcripts were aligned against the whole non-redundant database with a cut-off e-value of $<10^{-10}$. All unique transcript sequences were aligned against sequences in The Arabidopsis Information Resource (TAIR v.2.2.8) and the Universal Protein Resource Knowledgebase (UniProtKB) protein databases via the BLASTx algorithm. All sequences with blast hits were annotated with Gene Ontology (GO) terms by service providers at the National Research Council Plant Biotechnology Institute (NRC-PBI, Saskatoon, SK, Canada). Sequences were also assigned Kyoto Encyclopedia of Genes and Genomes (KEGG) annotations via the KEGG Automatic Annotation Server (KAAS) (Moriya et al., 2007).

Differential transcript expression was performed via RSEM algorithm and expression comparisons were based on $\log_2$ ratios of samples 2 and 3 to sample 1. Raw transcript expression data was obtained by service providers at the Plant Biotechnology Laboratory (University of Lethbridge) and raw read counts were received as a tab delimited file containing gene ID's, expression level and $\log_2$ ratios. Using GO and KEGG annotations all the genes involved with isoprenoid biosynthesis (DXP and MVA pathway as well as terpene synthase/cyclases) were identified and their differential expression patterns analyzed. The GO and KEGG annotations were also used to identify all photosynthetic genes (Supplementary Table S1) as well as fatty acid biosynthetic genes (Supplementary Table S4).

4.7. Monoterpene Synthase Candidate Selection

Two mTPS candidate genes, *CsγTRPS* and *CsLINS*, were chosen based on sequence homology to known mTPS genes, especially the presence of certain conserved motifs shared by all known TPS genes, DDXXD, (N,D)D(L,I,V)X(S,T)XXXE and RRX_8W, as well as one partially conserved motif, LQLYEASFLL. Protein sequence alignments between *CsγTRPS* and *CsLINS*, and *Citrus limon* γ-terpinene synthase, *Lavandula angustifolia* linalool synthase, *Salvia fruticosa* 1,8-cineole synthase, *Cannabis sativa* limonene synthase, *L. angustifolia* β-phellandrene synthase and *Salvia officinalis* sabinene synthase were performed with ClustalW2. Those transcripts with GO annotation "monoterpene biosynthetic process" as well as transcripts with BLASTx hits to known mTPS genes having an e-value $<10\text{-}^{60}$ were selected as coriander mTPS gene candidates.

4.8. Cloning of Full Length Monoterpene Synthase

The N-terminal signal peptide sequences of *CsγTRPS* and *CsLINS* were predicted using ChloroP (v.1.1). The open reading frame of *CsγTRPS* excluding the N-terminal signal peptide

was sticky end PCR amplified (Zeng, 1998) by Kapa HiFi DNA polymerase ready-mix (Kapa Biosystems Inc., Woburn, MA, USA). Sticky end primers (Supplementary Table S5) were designed to create EcoR1 and Xho1 (New England Biolabs, Whitby, ON, Canada) overhang regions for use during ligation of *CsγTRPS* into pET41b(+) bacterial expression vector (EMD Chemicals, Darmstadt, Germany). The PCR program used was as follows: 95 ^{o}C for 5 min, followed by 35 cycles of 98 ^{o}C for 20 sec, 60 ^{o}C for 15 sec and 72 ^{o}C for 1 min, and a 5 min final extension at 72 ^{o}C.

The *CsLINS* ORF, excluding the signal peptide, was amplified using the forward (5′- ACA CAT ATG ACT AAG GTT CCT GTT CCA GTA CCA G -3′) and reverse (5′-ATA AAG CTT GAG AGG AAT GGG CTC GAC AAG AAG-3′) primers in the same Kapa ready-mix. The Nde I and Hind III restriction enzyme (NEB) sites were designed into the forward and reverse primers (underlined), respectively. The PCR program used was 95 ^{o}C for 5 min, followed by 35 cycles of 95 ^{o}C for 1 min, 60 ^{o}C for 30 sec and 72 ^{o}C for 2 min, and a final extension at 72 ^{o}C for 5 min. The amplicons were purified with an E.Z.N.A DNA Purification Kit (Omega Bio-Tek, GA, USA) and each fused to a C-terminal eight histidine moiety in the pET41b(+) vector to facilitate downstream protein purification.

The CsLINS PCR product was digested with NdeI and HindIII as per manufacturer's protocol and the digested DNA was extracted from an agarose gel via the Omega Gel Extraction Kit (Omega). The fragment was ligated into pET41b(+) expression vector as was done with *CsγTRPS*.

4.9. Recombinant Protein Expression, Crude Enzyme Assay and Purification

The expression constructs were transformed via heat shock into *E. coli* Rosetta (DE3) pLysS expression cells (Novagen, Darmstadt, Germany). Successful transformants were selected on

solid Lauria-Bertani (LB) medium containing 30 µg/ml of kanamycin and 34 µg/ml of chloramphenicol. Single colonies were inoculated in 5 ml LB media with the same antibiotics and grown at 37 ^{o}C and 190 rpm for 14-16 hours. The 5 ml cultures were transferred to 95 ml LB media with antibiotics and incubated at 30 ^{o}C and 190 rpm until OD_{600} of ~0.8 was reached. Protein expression was induced by the addition of isopropyl-β-D-thiogalactopyranoside (IPTG) to a final concentration of 0.5 mM, and incubation at 18 ^{o}C and 190 rpm for 14-16 hours. Induced cells were split into two 50 ml portions and pelleted at 4 ^{o}C and 4000 rpm for 20 minutes before storage at -80 ^{o}C to lyse the cells.

For initial activity determination, frozen induced pellets were resuspended in 1 ml crude assay buffer (25 mM TRIS-Cl, 5% glycerol, 1 mM dithiothreitol (DTT), 10 mM $MgCl_2$ and 1 mM $MnCl_2$ at pH 7.5) (Crowell et al., 2002) supplemented with 1 mM proteinase inhibitor, phenylmethanesulfonylfluoride (PMSF). Cells were sonicated on ice for six 10 sec intervals with 1 min cool down periods using a Sonic Dismembrator Model 100 (Fisher Scientific, Ottawa, ON, Canada). The lysate was centrifuged at 14,000 rpm and 4 ^{o}C for 11 min to obtain the soluble protein fraction. One hundred microliters of crude soluble lysate was added to 2.9 ml of crude assay buffer with 25 µM geranyl diphosphate (GPP (**18**)) as substrate. The assay mixture was overlaid with 1 ml pentane to trap the volatile products and incubated in a 30 ^{o}C water bath for 2 hours. Following incubation, the assay was mixed vigorously and pentane overlay was removed for product analysis.

For purification, *E. coli* pellets containing CsγTRPS or CsLINS were resuspended in 5 ml Ni-NTA binding buffer (50 mM NaH_2PO_4, 300 mM NaCl and 10 mM imidazole at pH 8.0) supplemented with 1 mM PMSF. Cells were sonicated on ice for eight 15 sec intervals with 1 min cool down periods in between. The soluble fraction was collected by centrifugation at

10,500 rpm and 4 ^{o}C for 15 min. The His-tagged protein was then purified from the soluble lysate by Ni-NTA agarose affinity chromatography (EMD Chemicals, Germany) according to the manufacturer's protocol. The eluted CsLINS protein was further treated with an Amicon buffer exchange column (50 MWCO) to remove salts and dilute with protein storage buffer (50 mM tris, 1 mM EDTA, 1 mM DTT with 10% glycerol at pH 7.0).

Partially purified recombinant CsγTRPS and CsLINS, as well as soluble and insoluble total protein extracts from induced and non-induced *E. coli* cells was resolved with 12% sodium dodecyl sulfate polyacrylamide gel electrophoresis (SDS-PAGE) and visualized by Coomassie Brilliant Blue staining (Supplementary Figure S6 A and B). Total protein concentration was determined via the Bradford photometric method and protein quantitative analysis was performed by densitometry using Kodak 1D software (v. 3.6).

4.10. Pure/Semi-pure Enzyme Assays and Product Analysis

Assays were performed in 200 µl of the assay buffer (50 mM TRIS-Cl, 5% glycerol, 1 mM $MgCl_2$, 1 mM $MnCl_2$, 1 mg/ml Bovine Serum Albumin (BSA) and 1 mM DTT at pH 6.8) containing 25 µM of the GPP substrate (**18**) (Echelon, Salt Lake City, UT, USA) and 5-6 µg of the partially purified CsγTRPS and CsLINS proteins (75.90 pmol CsγTRPS; 87.23 pmol CsLINS). To study the linear kinetic properties of CsγTRPS, six time course points, 2.5, 5.0, 10, 15, 30 and 45 minutes were chosen; for CsLINS five time course points, 10, 20, 40, 60, and 90 minutes. Optimum temperature and pH were determined by assaying at various temperatures, 25, 27, 30, 32, 35 and 37 ^{o}C (CsγTRPS) and 25,27,30,32 and 35 ^{o}C (CsLINS), and six pH levels. The 2-(N-Morpholino) ethanesulfonic acid (MES) buffer maintained pH's 5.5, 6.0 and 6.5 while 3-Morpholino-2-hydroxypropanesulfonic acid (MOPSO) buffer maintained pH's 7.0, 7.5 and 8.0. Divalent cation preference and optimums for CsγTRPS were determined by assaying five

different $MnCl_2$ (Mn^{2+}) and $MgCl_2$ (Mg^{2+}) concentrations, 0.0025, 0.005, 0.25, 1.0, 5.0 mM and 2.0, 10.0, 50.0, 100.0, 250.0 mM, respectively. Negative control assays contained affinity purified protein extracted from Rosetta (DE3) pLysS *E. coli* cells which were transformed with "empty pET41b(+) vector" rather than construct containing gene of interest. For all assays two biological replicates and two technical replicates were prepared.

Volatile assay products were concentrated by exposure to a stream of pure helium gas, identified and quantified by GC-MS as previously described (Demissie et al., 2011) for EO analysis. To determine the stereoisomeric configuration of the linalool product, assay products were passed through the same GC coupled to a flame ionization detector (FID) detector. In this case the instrument was equipped with a 30 m x 0.25 mm fused silica capillary column coated with Chirasil-DEX (cyclodextrin directly bonded to dimethylpolysiloxane) (Agilent Technologies Canada Inc, Missisauga, ON, CAN). Samples were injected at 40 ^{o}C, and the oven temperature was initially maintained at 40 ^{o}C for 3 min, followed by a two-step temperature increase, first to 150 ^{o}C (at a rate of 10 ^{o}C per minute) and then to 230 ^{o}C (at a rate of 30 ^{o}C per minute), and held at 230 ^{o}C for 2 min. The carrier gas (helium) flow rate was set to 1 ml per minute.

All assay products were identified by comparison of their mass spectra to those in the National Institute of Standards and Technology (NIST) library database (NIST MS Search v.2.0), and by comparing their retention times and mass spectra to those of authentic standards (Sigma-Aldrich, Oakville, ON, CAN and Treatt, Lakeland, FL, USA). Terpene assay products were quantified by addition of 100 µl of 1 ppm camphor internal standard. All volatile enzyme assay extracts were GC analyzed with two technical replicates (two separate 2 µl injections).

Acknowledgements

We would like to thank David Arkinstall (University of British Columbia Okanagan SEMLab, Kelowna, BC, Canada) for his assistance with the scanning electron microscopy. In particular we are thankful to Dr. Slava Ilyntskyy and Dr. Igor Kovalchuk (Plant Biotechnology Laboratory, University of Lethbridge, Lethbridge, AB, Canada) for Illumina sequencing and *De novo* transcriptome assembly services. This work was supported through grants or in-kind contributions to Dr. Soheil Mahmoud by the University of British Columbia, Canada Foundation for Innovation, Natural Sciences and Engineering Research Council of Canada, and National Research Council of Canada.

Appendix A. Supplementary Data

Supplementary data associated with this article can be found, in the online version, at "hyperlink".

Figures

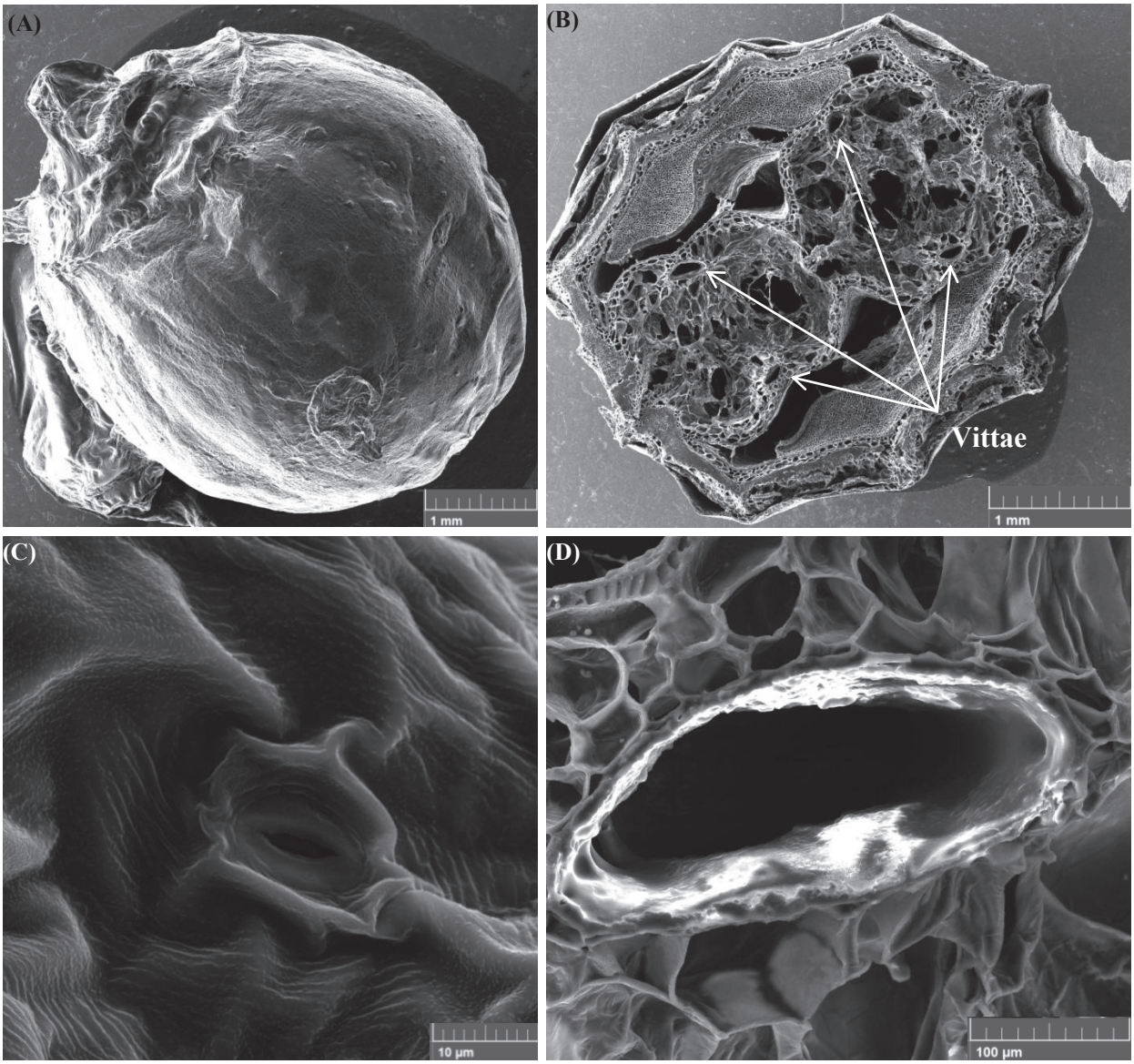

Fig. 1.

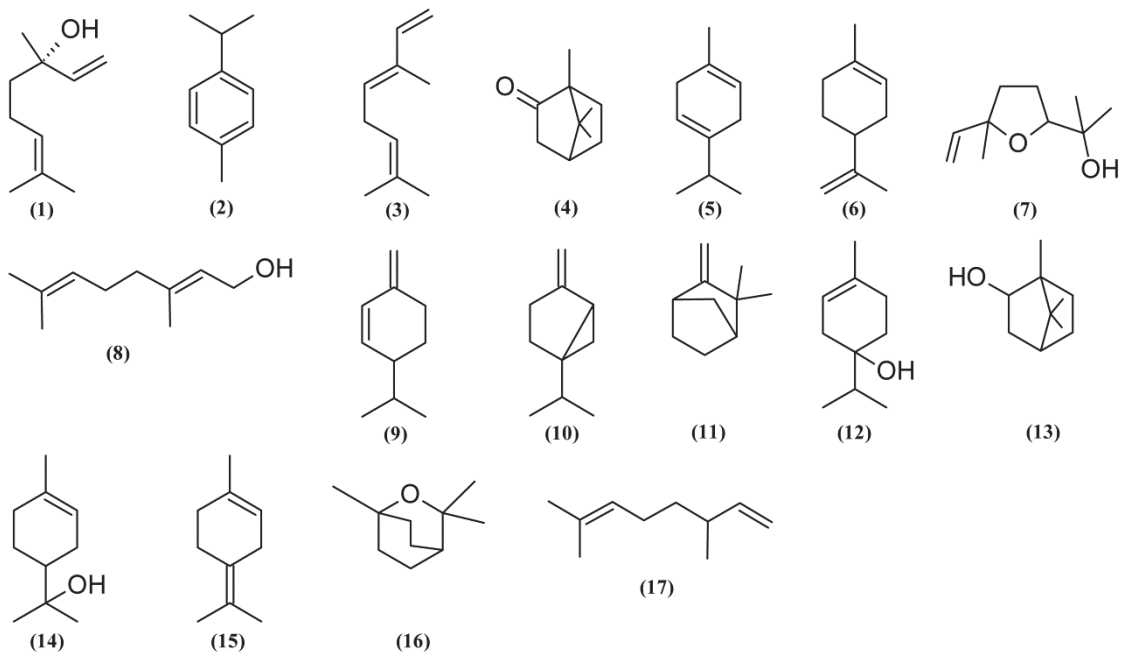

Fig. 2.

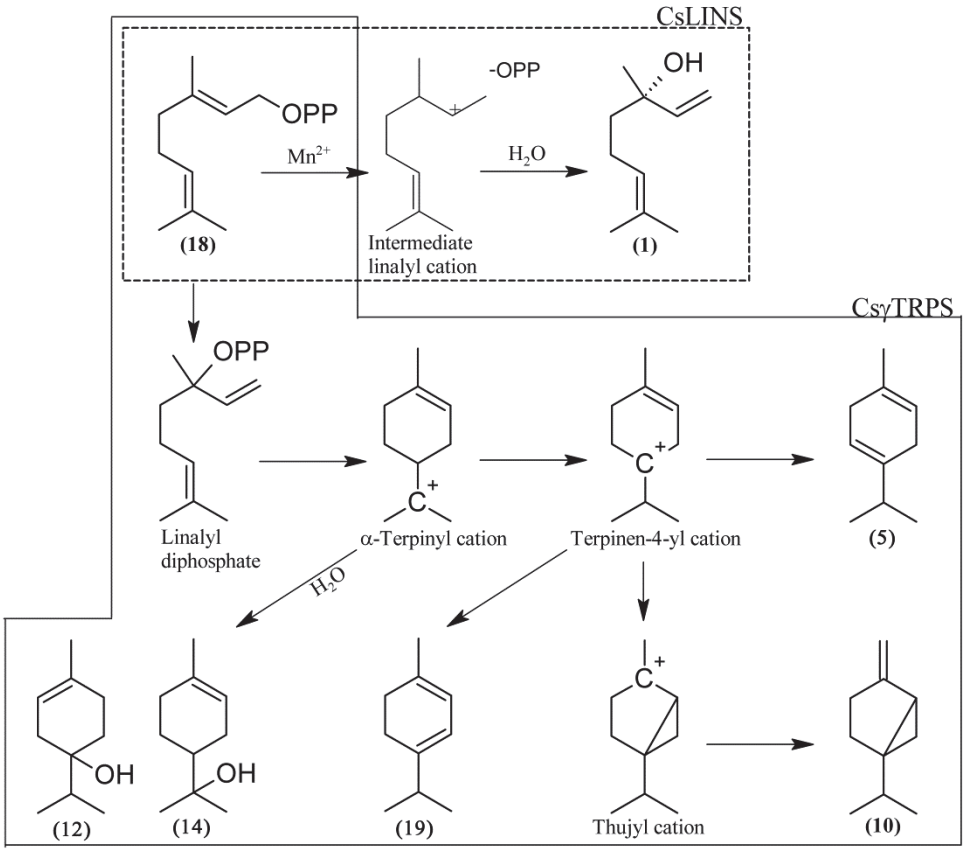
CsLINS
OPP
Mn2+
-OPP
H2O
OH
(18)
Intermediate
linalyl cation
(1)
CsγTRPS
OPP
Linalyl
diphosphate
α-Terpinyl cation
Terpinen-4-yl cation
(5)
H2O
OH
OH
(12)
(14)
(19)
Thujyl cation
(10)

Fig. 3.

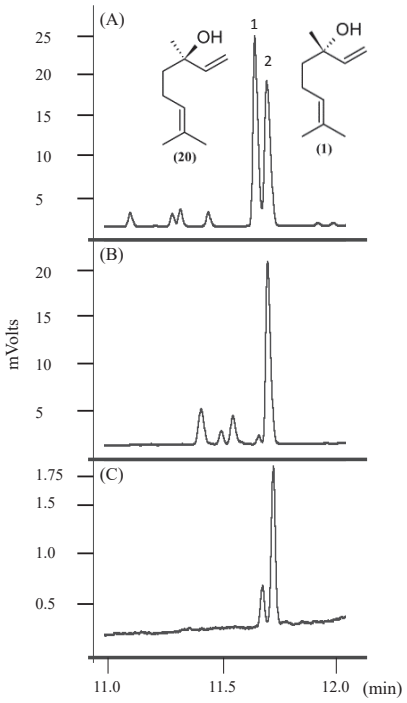
(A)
OH
1
2
OH
(20)
(1)
25
20
15
10
5
(B)
20
15
10
5
mVolts
1.75
(C)
1.5
1.0
0.5
11.0
11.5
12.0
(min)

Fig. 4.

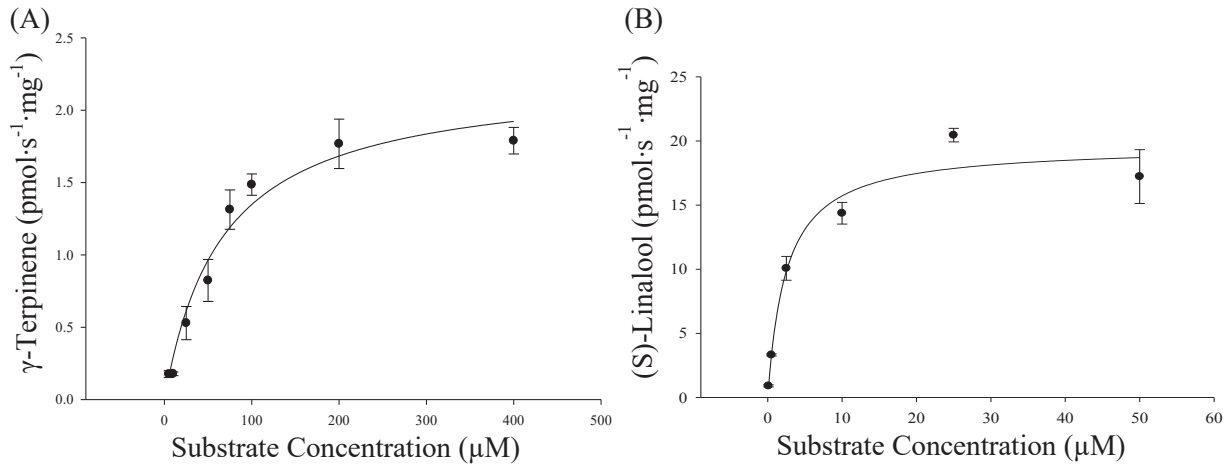

Fig. 5.

Figure legends

Figure 1. Scanning electron microscope images of *C. sativum* mericarp tissue. **(A)** Whole mericarp, **(B)** cross-section with four vittae visible, **(C)** stomata on mericarp surface, **(D)** close-up of a vitta.

Figure 2. Structures for volatile terpenes found in *C. sativum* mericarps use in this study.

Figure 3. Conversion of geranyl diphosphate to (S)-linalool by CsLINS, and to other monoterpene products by CsγTRPS.

Figure 4. Gas chromatogram using chiral column to separate (S)-linalool (**1**) and (R)-linalool (**20**). (A) (S/R)-Linalool stereoisomer blend standard (peak 1 is (R)- and peak 2 is (S)-linalool, (B) (S)-linalool standard and (C) CsLINS with geranyl diphosphate assay product.

Figure 5. Kinetics data for CsγTRPS (A) and CsLINS (B) with GPP substrate. Each enzymatic assay consisted of two biological and two technical replicates. CsγTRPS and CsLINS proteins catalyzed the conversion of geranyl diphosphate to γ-terpinene and (S)-linalool, respectively,

with apparent V_{max} and K_m values of 2.24 ± 0.16 (CsγTRPS) and 19.63 ± 1.05 (CsLINS) pkat/mg, and 66.25 ± 13 (CsγTRPS) and 2.5 ± 0.6 (CsLINS) μM, respectively.

Tables

Table 1 Coriander mericarp essential oil (EO) terpene composition. Error bounds are in percent standard deviation.

Terpene	% of Total EO
(S)-Linalool (**1**)	78.96 ± 2.86
Cymene (**2**)	6.38 ± 1.28
Ocimene (**3**)	4.46 ± 3.39
Camphor (**4**)	3.62 ± 0.38
γ-Terpinene (**5**)	2.66 ± 1.34
Limonene (**6**)	1.13 ± 0.04
Linalool oxide (**7**)	1.10 ± 0.25
Geraniol (**8**)	0.67 ± 0.54
β-phellandrene (**9**)	0.50 ± 0.14
Sabinene (**10**)	0.48 ± 0.41
Camphene (**11**)	0.32 ± 0.05
Terpinen-4-ol (**12**)	0.25 ± 0.09
Borneol (**13**)	0.18 ± 0.14
α-Terpineol (**14**)	0.18 ± 0.15
Terpinolene (**15**)	0.13 ± 0.05
1,8-Cineole (**16**)	tr
Citronellene (**17**)	tr

* "tr" indicates trace amounts detected (<0.1%)

Table 2 Transcript abundance for putative genes involved in coriander isoprenoid biosynthesis across three stages of mericarp development (S1, S2, S3).

	RPKM-Normalized Counts				
	S1	S2	S3	$\log_2$(S2/S1)	$\log_2$(S3/S1)
Monoterpene biosynthesis					
(S)-Linalool synthase	3015	7317	1350	1.279	-1.160
mTPS2	4110	3829	3962	-0.1022	-0.0529
γ-Terpinene synthase	664	1645	715	1.309	0.1070
mTPS3	502	255	847	-0.9787	0.7546
Sesqui- and Triterpene biosynthesis					
Squalene monooxygenase3	589	551	503.01	-0.0962	-0.2277
Squalene monooxygenase1	333	419	350	0.3314	0.0718
Squalene monooxygenase2	158	209	183	0.4036	0.2119
Squalene synthase	750	1061	764	0.5005	0.0267
sTPS1	1127	3177	631	1.495	-0.8368
sTPS2	578	1056	466	0.8694	-0.3107
Brassinosteroids	438	694	579	0.6643	0.4018
Diterpene biosynthesis					
ent-Kaurene acid hydroxylase	502	348	494	-0.5301	-0.0221
Gibberellin 2-oxidase1	201	37	174	-2.442	-0.2081
ent-Kaurene oxidase	191	275	147	0.5259	-0.3812
ent-Kaurene synthase	150	180	136	0.2630	-0.1414
Gibberellin 2-oxidase2	91	409	104	2.168	0.1978
Gibberellin 3-β-dioxygenase	493	609	226	0.3047	-1.125
Tetraterpene biosynthesis					
9-cis- Epoxycarotenoid dioxygenase	108	20	44	-2.441	-1.298
Lycopene ε-cyclase	468	385	323	-0.2817	-0.5350
Prolycopene isomerase	472	457	471	-0.0466	-0.0031
ζ-Carotene isomerase	85	171	105	1.008	0.3049
Xanthoxin dehydrogenase	390	472	349	0.2763	-0.1607
(+)-Abscisic acid 8-hydroxylase	54	105	48	0.9594	-0.1699
ζ-Carotene desaturase	663	799	907	0.2692	0.4521
Zeaxanthin epoxidase	716	570	1312	-0.3290	0.8741
Violaxanthin de-epoxidase	265	262	455	-0.0164	0.7801
Lycopene β-cyclase	254	332	418	0.3864	0.7187
15-cis-Phytoene desaturase	813	950	1035	0.2249	0.3483
Abscisic-aldehyde oxidase	342	275	411	-0.3128	0.2663
β-carotene 3-hydroxylase	202	109	280	-0.8953	0.4702
Phytoene synthase	422	270	499	-0.6443	0.2418

Table 3 Kinetics properties of coriander γ-terpinene synthase and (S)-linalool synthase with the GPP substrate.

	CsγTRPS	CsLINS
K_m	66.25 ± 13.32 μM	2.5 ± 0.6 μM
V_{max}	2.24 ± 0.16 p_{kat}/mg	19.63 ±1.05 p_{kat}/mg
k_{cat}	1.476×10^{-4} s^{-1}	1.4×10^{-3} s^{-1}
k_{cat}/K_m	2.228×10^{-6} $s^{-1}\mu M^{-1}$	5.4×10^{-4} $s^{-1}\mu M^{-1}$

References

Bakkali, F., Averbeck, S., Averbeck, D., Waomar, M. 2008. Biological effects of essential oils - A review. Food Chem. Toxicol. 46, 446-475.

Barrett, T., Suzek, T. O., Troup, D. B., Wilhite, S. E., Ngau, W. C., Ledoux, P., Rudenv, D., Lash, A. E., Fugibuchi, W., Edgar, R. 2005. NCBI GEO: Mining millions of expression profiles - database and tools. Nucleic Acids Res. 33, D562-D566.

Benveniste, P. 2004. Biosynthesis and accumulation of sterols. Annu. Rev. Plant Biol. 55, 429-457.

Bhuiyan, N., I., Begum, J., and Sultana, M. 2009. Chemical composition of leaf and seed essential oil of *Coriandrum sativum* L. from Bangladesh. Bangladesh J. Pharmacol. 4, 150-153. Chithra, V., Leelamma, S. 2000. *Coriandrum sativum* - effect on lipid metabolism in 1,2-dimethyl hydrazine induced colon cancer. J. Ethnopharmacol. 71, 457-463.

Clouse, S., Sasse, J. 1998. Brassinosteroids: Essential regulators of plant growth and development. Annu. Rev. Plant Physiol. Plant Mol. Biol. 49, 427-451.

Croteau, R., Kutchan, T.M., Lewis, N.G. 2000. Natural Products (Secondary Metabolites), In Biochemistry and Molecular Biology of Plants, Buchanan, B., Gruissem, W., and Jones, R., eds (Rockville: American Society of Plant Physiologists), pp. 1250-1277.

Crowell, A., Williams, D., Davis, E., Wildung, M., Croteau, R. 2002. Molecular cloning and characterization of a new linalool synthase. Arch. Biochem. Biophys. 405, 112-121.

Demissie, Z.A., Sarker, L.S., Mahmoud, S.S. 2011. Cloning and functional characterization of beta-phellandrene synthase from *Lavandula angustifolia*. Planta. 233, 685-696.

Dewick, P.M. 2001. Medicinal natural products: a biosynthetic approach, second edition. (Hoboken: Wiley), pp. 167-289.

Dhanapakiam, P., Joseph, J.M., Ramaswamy, V.K., Moorthi, M., Kumar, A.S. 2008. The cholesterol lowering property of coriander seeds (*Coriandrum sativum*): Mechanism of action. J. Environ. Biol. 29, 53-56.

Gallagher, A., Flatt, P., Duffy, G., Abdel-Wahab, Y. 2003. The effects of traditional antidiabetic plants on in vitro glucose diffusion. Nutr. Res. 23, 413-424.

Ganjewala, D., Kumar, S., Luthra, R. 2009. An account of cloned genes of methyl-erythritol-4-phosphate pathway of isoprenoid biosynthesis in plants. Current Issues in Molecular Biology. 11, 35-45.

Garg, R., Patel, R.K., Tyagi, A.K., Jain, M. 2011. De novo assembly of chickpea transcriptome using short reads for gene discovery and marker identification. DNA Res. 18, 53-63.

Gross, M., Joel, D.M., Cohen, Y., Bar, E., Friedman, J., and Lewinsohn, E. 2006. Ontogenesis of mericarps of bitter fennel (*Foeniculum vulgare* mill. var. vulgare) as related to t-anethole accumulation. Isr. J. Plant Sci. 54, 309-316.

Hasunuma, T., Takeno, S., Hayashi, S., Sendai, M., Bambi, T., Yoshimura, S., Tomizawa, K., Fukusaki, E., and Miyake, C. 2008. Overexpression of 1-deoxy-D-xylulose-5-phosphate reductoisomerase gene in chloroplast contributes to increment of isoprenoid production. J. Biosci. Bioeng. 105, 518-526.

Hemmerlin, A., Hoeffler, J. F., Meyer, O., Tritsch, D., Kagan, I. A., Grosdemagne-Billard, C., Rohmer, M., and Bach, T. J. 2003. Cross-talk between the cytosolic mevalonate and the plastidial methylerythritol phosphate pathways in tobacco bright yellow-2 cells. J. Biol. Chem. 278, 26666-26676.

Jernstedt, J., Clark, C. 1979. Stomata on the fruits and seeds of *Eschscholzia* (papaveraceae). Am. J. Bot. 66, 586-590.

Kubo, I., Fujita, K., Kubo, A., Nihei, K., Ogura, T. 2004. Antibacterial activity of coriander volatile compounds against *Salmonella choleraesuis*. J. Agric. Food Chem. 52, 3329-3332.

Lane, A., Boecklemann, A., Woronuk, G.N., Sarker L.S., Mahmoud, S.S. 2010. A genomics resource for investigating regulation of essential oil production in *Lavandula angustifolia*. Planta. 231 (4), 835-845.

Li, C., Zhu, Y., Guo, X., Sun, C., Luo, H., Song, J., Li, Y., Wang, L., Qian, J., and Chen, S. 2013. Transcriptome analysis reveals ginsenosides biosynthetic genes, microRNAs and single sequence repeats in *Panax ginseng* C. A. meyer. BMC Genomics. 14, 245-255.

Li, X., Acharya, A., Farmer, A. D., Crow, J. A., Bharti, A. K., Kramer, R. S., Wei, Y., Han, Y., Gou, J., May, G. D., Monteros, M. J., and Brummer, E. C. 2012. Prevalence of single nucleotide polymorphism among 27 diverse alfalfa genotypes as assessed by transcriptome sequencing. BMC Genomics. 13, 568-579.

Lo Cantore, P., Lacobellis, N., De Marco, A., Capasso, F., Senatore, F. 2004. Antibacterial activity of *Coriandrum sativum* L. and *Foeniculum vulgare* miller var. *vulgare* (miller) essential oils. J. Agric. Food Chem. 52, 7862-7866.

Lupien, S., Karp, F., Wildung, M., and Croteau, R. 1999. Regiospecific cytochrome P450 limonene hydroxylases from mint (*Mentha*) species: CDNA isolation, characterization, and functional expression of (-)-4S-limonene-3-hydroxylase and (-)-4S-limonene-6-hydroxylase. Arch. Biochem. Biophys. 368, 181-192.

Mahendra, P., Bisht, S. 2011. Anti-anxiety activity of *Coriandrum sativum* assessed using different experimental anxiety models. Indian J. Pharmacol. 43, 574-577.

Mahmoud, S.S., Croteau, R.B. 2002. Strategies for transgenic manipulation of monoterpene biosynthesis in plants. Trends Plant Sci. 7, 366-373.

Maluf, M., Saab, I., Wurtzel, E., Sachs, M. 1997. The viviparous12 maize mutant is deficient in abscisic acid, carotenoids, and chlorophyll synthesis. J. Exp. Bot. 48, 1259-1268.

Martin, D., Faldt, J., Bohlmann, J. 2004. Functional characterization of nine norway spruce TPS genes and evolution of gymnosperm terpene synthases of the TPS-d subfamily. Plant Physiol. 135, 1908-1927.

Misharina, T. 2001. Influence of the duration and conditions of storage on the composition of the essential oil from coriander seeds. Appl. Biochem. Microbiol. 37, 622-628.

Moriya, Y., Itoh, M., Okuda, S., Yoshizawa, A., Kanehisa, M. 2007. KAAS: An automatic genome annotation and pathway reconstruction server. Nucleic Acids Res. 35, 182-185.

Msaada, K., Hosni, K., Ben Taarit, M., Ouchikh, O., Marzouk, B. 2009a. Variations in essential oil composition during maturation of coriander (*Coriandrum sativum* L.) fruits. J. Food Biochem. 33, 603-612.

Msaada, K., Hosni, K., Ben Taarit, M., Chahed, T., Hammami, M., Marzouk, B. 2009b. Changes in fatty acid composition of coriander (*Coriandrum sativum* L.) fruit during maturation. Ind. Crop. Prod. 29, 269-274.

Munoz-Bertomeu, J., Arrillaga, I., Ros, R., Segura, J. 2006. Up-regulation of 1-deoxy-D-xylulose-5-phosphate synthase enhances production of essential oils in transgenic spike lavender. Plant Physiol. 142, 890-900.

Okamoto, S., Yu, F., Harada, H., Okajima, T., Hattan, J., Misawa, N., and Utsumi, R. 2011. A short-chain dehydrogenase involved in terpene metabolism from zingiber zerumbet. Febs Journal. **278,** 2892-2900.

Page, R. 1996. TreeView: An application to display phylogenetic trees on personal computers. Comput. Appl. Biosci. 12, 357-358.

Paiva, E., Lemos, J., Oliveira, D. 2006. Imbibition of *Swietenia macrophylla* (meliaceae) seeds: The role of stomata. Ann. Bot. 98, 213-217.

Parthasarathy, V.A., Zachariah, T.J. 2008. Coriander, In Chemistry of Spices, Parthasarathy, V.A., Chempakam, B., and Zachariah, T.J. (London, UK: CAB International), pp. 190-210.

Pichersky, E., Lewinsohn, E., Croteau, R. 1995. Purification and characterization of S-linalool synthase, an enzyme involved in the production of floral scent in *Clarkia-breweri*. Arch. Biochem. Biophys. 316, 803-807.

Potter, T. 1996. Essential oil composition of cilantro. J. Agric. Food Chem. 44, 1824-1826.

Poulose, A., and Croteau, R. 1978. Biosynthesis of aromatic monoterpenes - conversion of gamma-terpinene to para-cymene and thymol in *Thymus vulgaris* L1. Arch. Biochem. Biophys. 187, 307-314.

Purseglove, J.W., Brown, E.G., Green, C.L., Robbins, S.R.J. 1981. Spices, vol. 2. (London: Longman), pp. 736-788.

Ramadan, M., and Morsel, J. 2002. Oil composition of coriander (*Coriandrum sativum* L.) fruit-seeds. Eur. Food Res. Technol. 215, 204-209.

Reuter, J., Huyke, C., Casetti, F., Theek, C., Frank, U., Augustine, M., and Schempp, C. 2008. Anti-inflammatory potential of a lipolotion containing coriander oil in the ultraviolet erythema test. J. Dtsch. Dermatol. Ges. **6,** 847-851.

Rodriguez-Concepcion, M. 2010. Supply of precursors for carotenoid biosynthesis in plants. Arch. Biochem. Biophys. 504, 118-122.

Rugenstein, S., Lersten, N. 1981. Stomata on seeds and fruits of *Bauhinia* (leguminosae, caesalpinioideae). Am. J. Bot. 68, 873-876.

Sarker, L.S., Galata, M., Demissie, Z.A., Mahmoud, S.S. 2012. Molecular cloning and functional characterization of borneol dehydrogenase from the glandular trichomes of *lavandula x intermedia*. Arch. Biochem. Biophys. 528, 163-170.

Sriti, J., Talou, T., Wannes, W.A., Cerny, M., and Marzouk, B. 2009. Essential oil, fatty acid and sterol composition of Tunisian coriander fruit different parts. J. Sci. Food Agric. 89**,** 1659-1664.

Tschiersch, H., Borisjuk, L., Rutten, T., Rolletschek, H. 2011. Gradients of seed photosynthesis and its role for oxygen balancing. BioSystems. 103, 302-308.

Turner, G.W., Croteau, R. 2004. Organization of monoterpene biosynthesis in *Mentha*. immunocytochemical localizations of geranyl diphosphate synthase, limonene-6-hydroxylase, isopiperitenol dehydrogenase, and pulegone reductase. Plant Physiol. 136, 4215-4227.

Valasek, M., Repa, J. 2005. The power of real-time PCR. Adv. Physiol. Educ. 29, 151-159.

Vonheijne, G., Steppuhn, J., and Herrmann, R. 1989. Domain-structure of mitochondrial and chloroplast targeting peptides. Eur. J. Biochem. 180, 535-545.
Werker, E. 1997. Seed anatomy (Berlin: Gerbrüder-Borntraeger), pp. 50-54.
Wu, H., Hu, Z. 1997. Comparative anatomy of resin ducts of the *Pinaceae*. Trees-Struct. Funct. 11, 135-143.
Yazaki, K. 2006. ABC transporters involved in the transport of plant secondary metabolites. FEBS Lett. 580, 1183-1191.
Zeng, G. 1998. Sticky-end PCR: New method for subcloning. BioTechniques. 25, 788.